Supplementary Material (ESI) for Lab on a Chip

Supplementary material for supercooled micro flows and application for asymmetric synthesis

Shinya Matsuoka[a], Akihide Hibara[a,b,c], Masaharu Ueno[a,b,c],, Takehiko Kitamori*[a,b,c]

[a] *Department of Applied Chemistry, School of Engineering, The University of Tokyo, 7-3-1 Hongo, Bunkyo, Tokyo 113-8656, Japan. Fax: +81-3-5841-6039; E-mail: kitamori@icl.t.u-tokyo.ac.jp*
[b] *Japan Science and Technology Agency, 4-1-8 Honcho, Kawaguchi, 332-0012, Japan.*
c Micro Chemistry Group, Kanagawa Academy of Science and Technology, 3-2-1 Sakado, Takatsu, Kawasaki, 213-0012, Japan.

1. Microchips and temperature control

Pyrex glass microchips were purchased from the Institute of Microchemical Technology (Kawasaki, Japan). Fabrication schemes were presented previously. For investigation of fundamental properties of the supercooled state including its size dependence, we used six microchips having 60-mm-long straight microchannels (ICC-DI05, Fig. S1) of different widths and depths. The widths and depths are summarized in Table S1. For the asymmetric synthesis, a microchip having a long reaction microchannel with y-shaped junction after confluence of two inlet microchannels was used (ICC-KG01, Fig. 2a of the body). The width and depth of the reaction microchannel were 200 μm and 100 μm, respectively, and length of reaction part was 50 cm.

The microchips were put on a temperature controlling stage (LST350, Linkam Scientific Instruments, Waterfield, UK), which can control the microchip temperature from -190 ºC to 300 ºC by circulating liquefied nitrogen and electrically heating (Fig. S2).

In order to ensure that water temperature inside the microchannels was the same as that displayed on the driver of the temperature control stage (Figure S2), we confirmed the temperature of the microchip top surface, which was in contact with room-temperature air by measuring it with a radiation thermometer. The microchip bottom surface was in contact with the temperature control stage and we confirmed that the top surface temperature followed the stage temperature. The delay time between the two temperatures was within 10 s.

Next, the temperature change inside the reaction microchannel (200-μm width and 100-μm depth) was numerically calculated. Initially, temperatures of water and glass substrate were set to 25 °C and -20 °C, respectively. The calculation results showed that the temperature of water decreased to the substrate temperature (-20 °C) within 6 s. Since a typical flow rate of 1 μl/min corresponds to 1 mm/s for the above-sized microchannel, the liquid temperature reached the setting temperature within several millimeters of entering the long reaction microchannel.

Furthermore, the water temperature was measured experimentally by using a micro thermocouple inserted from a hole drilled into the side of the microchip. This measured water temperature agreed with that of the stage within experimental error of less than 1 °C. From these results, we concluded that the temperature displayed on the driver of the control stage can be regarded as liquid temperature inside the microchannel.

Table S1 Dimensions of the microchips for investigation of fundamental properties of the supercooled state.

Microchip #	Width (μm)	Depth (μm)
1	70	30
2	100	40
3	120	60
4	190	90
5	240	120
6	300	150

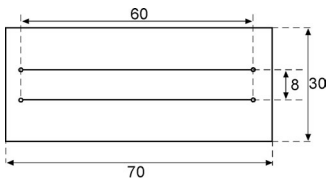

Fig. S1 Layouts of microchannels. (a) Simple straight microchannel for investigating fundamental properties of supercooled state of water.

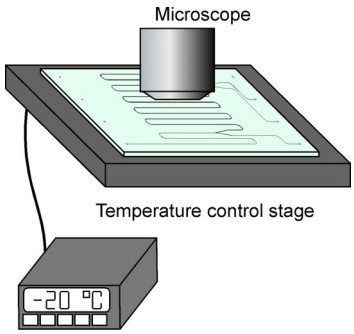

Fig. S2 Illustration of experimental setup. The microchip is fixed on a temperature control stage, and liquid in the microchannel is observed by a microscope.

2. Freezing point detection

In order to detect the freezing point of water in the microchannel, optical microscope images were analyzed. When the microchannel was filled with water, it was very difficult to distinguish whether water stayed in the liquid phase or solidified in places where no cracks were observed after solidification. Since refractive indexes of water and ice are 1.33 and 1.31, respectively, we had to analyze this slight difference. Figures S3a and S3b show typical micrographs before and after solidification, respectively. In these micrographs, the microchannel having a 100-μm width and 40-μm depth was used and water temperature was set to -15 °C.

In the microchannel just around the microchannel wall, a dark area was observed. The microchannel had a cross section approximating to a semicircular geometry and transmitted illumination light was induced from the curved surface of the microchannel as shown in Fig. S3c. Since the refractive index of glass is higher than that of water and ice, some part of the illumination light cannot be transmitted around the microchannel wall part because of the total internal reflection as predicted by Snell's law. Therefore, contrast of the dark area changes slightly after solidification.

In order to emphasize the slight refractive index change, we analyzed temporal change of the light intensity along the x-axis that was drawn in Fig. S3b. The light intensity at position x at a given time t was defined as $I(x, t)$, and the light intensity change $I(x, t)$–$I(x, t-\Delta t)$ is plotted in Figure S3d. In this case, no changes were observed except at 409 s. This change corresponded to freezing (solidification). When freezing was not detected at the setting temperature during 10 min (600 s), the temperature was increased to room temperature, and then decreased to the next setting point.

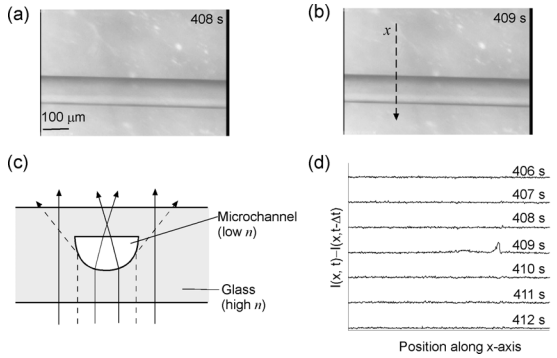

Fig. S3 Micrographs of microchannels filled with pure water (a) before and (b) after freezing. The times presented on the top-right correspond to observation time after the stage temperature reaches the setting temperature. (c) Illustration of locus of transmitted light through the microchannel section. A dark region is observed around the edge of the microchannel due to total internal reflection. (d) Light intensity change as a function of the observation time. Light intensity difference due to freezing is observed in the plot of 409 s.

3. Asymmetric reaction

N-(diphenylmethylene)glycine tert-butyl ester (D2322, Tokyo Kasei Kogyo, Tokyo, Japan), the alkylation reagent benzyl bromide (B0411, Tokyo Kasei Kogyo, Tokyo, Japan), and the PTC of (S,S)-3,4,5-trifluorophenyl-NAS bromide (Aldrich-548383, Sigma-Aldrich Japan, Tokyo, Japan) were used without further purification. All water used in these experiments was diluted, deionized and filtered through a membrane filter (pore size 0.2 μm).

The microchip shown in Fig. 2a of the body, which has a Y-shaped junction and 50-cm long reaction microchannel, was used for the reaction. A dichloromethane solution of ester (0.5 M), alkylation reagent (0.6 M) and chiral PTC (0.05M) made up the organic phase and aqueous KOH (1.0 M) was used as the aqueous phase. Organic and aqueous phases were introduced from separate inlets into the reaction microchannel at the flow rate of 1.0 μl/min. After the Y-junction point, the two-phase flow formed segmented flow. The asymmetric reaction was carried out at controlled temperature. The output solution was collected in a microtube containing 0.5 ml hexane and 0.5 ml brine to quench the reaction by dilution. The collected organic phase was washed with water three times and dried with sodium sulfate. The enatiomeric excesses (ee) and reaction conversion were determined by HPLC analysis by using a chiral separation column (Chiralcel OD-H, Daisel Chemical Industries, Osaka, Japan).